Journal of Analytical and Applied Pyrolysis 100 (2013) 145–152

Contents lists available at SciVerse ScienceDirect

Journal of Analytical and Applied Pyrolysis

journal homepage: www.elsevier.com/locate/jaap

Intrinsic kinetics and devolatilization of wheat straw during torrefaction

Lei Shang[a,*], Jesper Ahrenfeldt[a], Jens Kai Holm[b], Søren Barsberg[c], Rui-zhi Zhang[d], Yong-hao Luo[d], Helge Egsgaard[a], Ulrik B. Henriksen[a]

[a] Department of Chemical and Biochemical Engineering, Technical University of Denmark, 2800 Kgs., Lyngby, Denmark
[b] Chemical Engineering, DONG Energy Thermal Power A/S, Nesa Alle 1, 2820 Gentofte, Denmark
[c] Biomass and Ecosystem Science, Faculty of Life Sciences, University of Copenhagen, Rolighedsvej 23, 1958 Frederiksberg, Denmark
[d] School of Mechanical Engineering, Shanghai Jiaotong University, Shanghai 200240, China

ARTICLE INFO

Article history:
Received 27 September 2012
Received in revised form
22 November 2012
Accepted 11 December 2012
Available online 24 December 2012

Keywords:
Torrefaction
Kinetics
TGA-MS
Wheat straw

ABSTRACT

Torrefaction is a mild thermal treatment (200–300 °C) in an inert atmosphere, which is known to increase the energy density of biomass by evaporating water and a proportion of volatiles. In this work, the degradation kinetics and devolatilization of wheat straw was studied in a thermogravimetric analyzer by coupling with a mass spectrometer. The kinetic parameters obtained by applying a two-step reaction in series model and taking initial dynamic heating period into account can accurately describe the experimental results with different heating programs. Activation energies and pre-exponential parameters obtained for the two steps are: 71.0 and 76.6 kJ mol^{-1}, 3.48 × 10^4 and 4.34 × 10^3 s^{-1}, respectively. The model and these parameters were also proven to be able to predict the residual mass of wheat straw in a batch scale torrefaction reactor. By analyzing the gas products in situ, the formation of water, carbon monoxide, formic acid, formaldehyde, methanol, acetic acid, carbon dioxide, methyl chloride, traces of hydrogen sulfide and carbonyl sulfide were found at torrefaction temperatures of 250 and 300 °C.

© 2012 Elsevier B.V. All rights reserved.

1. Introduction

Torrefaction is a mild temperature (200–300 °C) pretreatment in an inert atmosphere to upgrade ligno-cellulosic biomass to a high quality biofuel. During the process, biomass releases water and a part of the volatiles, causing a decrease in mass but an increase in energy density [1–3]. Our earlier work also showed improved grindability of wheat straw torrefied above 200 °C [3]. The loss of hemicelluloses, the degradation of which starts at 200–250 °C and cease at about 300 °C, is the main reason for the improvement of grindability in this temperature range. Degradation of the other two main components, lignin and cellulose, detected by ATR (attenuated total reflectance) – Fourier transform infrared spectroscopy occurs at 270–300 °C. This results in a higher energy loss from the wheat straw in this temperature range. So in order to control and optimize the process, it is desired to know the residence times required for complete conversion of the hemicelluloses but only minor degradation of cellulose and lignin in the biomass. The residence time is the result of heat, mass transfer and solid degradation rate in the reacting environment [4]. Therefore, it is important to know the chemical kinetics to predict the thermal decompositions of wheat straw. Thermogravimetric analysis (TGA) is the most common technique in solid-phase thermal degradation studies [5–7]. However, the use of TGA to determine kinetic parameters for the thermal degradation of biomass is complicated in that TGA only provides general information on the overall reaction kinetics while biomass decomposition represents a number of reactions in parallel and series. In practice, the aim of the kinetic evaluation of the thermogravimetric data is to obtain relatively simple models, describing the torrefaction of biomass [8]. There are plenty of research data [9] relating to pyrolysis of biomass under both dynamic conditions (non-isothermal) and steady-state (isothermal) conditions. The main advantage of determining kinetic parameters by non-isothermal methods rather than by isothermal studies is that only a single sample is required to calculate the kinetics over an entire temperature range in a continuous manner. However, it is widely agreed that multiple heating rates should be adopted to enhance the accuracy of the non-isothermal method [9].

In case of torrefaction, all kinetic studies [10–12] were conducted under isothermal condition. Prins et al. [12] used a two-step reaction in series model to describe the weight loss kinetics of willow torrefaction. This model, as shown in scheme (1), was earlier introduced by Di Blasi and Lanzetta [4] for studying the intrinsic kinetics of isothermal xylan degradation under inert atmosphere in the temperature range of 200–340 °C. They found that a one-step global reaction did not fit the experimental results satisfactorily, as the time derivative of the solid mass fraction as a function of temperature exhibited a double peak. In both steps, a competitive

---

[*] Corresponding author. Tel.: +45 2132 4979; fax: +45 4677 4109.
E-mail address: lesh@kt.dtu.dk (L. Shang).

0165-2370/$ – see front matter © 2012 Elsevier B.V. All rights reserved.
http://dx.doi.org/10.1016/j.jaap.2012.12.010

volatile and solid formation was taken into account. In the later study done by Branca and Di Blasi on beech wood [13], it was suggested that the first step is due to the degradation of extractives and the most reactive fractions of hemicelluloses, and the second step is due to the degradation of cellulose and part of lignin and hemicelluloses. For temperatures higher than 327 °C there is a third step, which can be attributed to the degradation of lignin and small fractions of the other two constituents. It was observed from both studies that the first step is much faster than the second step. Di Blasi and Lanzetta [4] pointed out the usual limitation encountered in order to attain the isothermal stage is that by using slow heating rates to avoid intra-particle temperature gradients usually result in non-negligible weight loss in the heating stage. Therefore high heating rate (40–70 °C s^{-1}) was adopted, and the char yield was determined as a function of the sample size prior to the tests to ensure no influence from the temperature spatial gradients. Constant char yields were attained for sample thickness around 100 μm, so particle size of 50 μm was chosen for the test. The results showed that the faction of mass loss for the beginning of isothermal stage is in the range of 0–0.16. So it was decided that these data can be analyzed by an isothermal model.

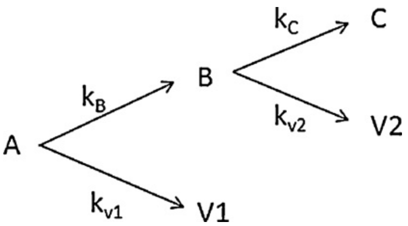

(1)

$$\frac{d[A]}{dt} = -(k_B + k_{v1})[A] \tag{2}$$

$$\frac{d[B]}{dt} = k_B[A] - (k_C + k_{v2})[B] \tag{3}$$

$$\frac{d[C]}{dt} = k_C[B] \tag{4}$$

In scheme (1) the xylan is denoted '*A*', and '*B*' is the intermediate compound, which is a solid with a reduced degree of polymerization. '*V1*' and '*V2*' are volatiles; '*C*' is the solid residue. From the proposed model, rate equations, as shown in Eqs. (2)–(4), can be obtained for solids by assuming first order reactions [4,12], where k is the rate constant for each step, and is expressed as s^{-1}. Integrate the above differential equations, with the initial condition that only A is present at the beginning of the reactions, expression for the solid residual, M, as a function of the two steps of the reaction mechanism can be given:

$$\frac{M - M_\infty}{M_0} = \lambda_1 e^{-K_1 t} + \lambda_2 e^{-K_2 t} \tag{5}$$

where

$$\frac{M}{M_0} = [A] + [B] + [C] \tag{6}$$

$$\lambda_1 = 1 + \left[\frac{k_B \cdot K_1 - k_B \cdot k_C}{K_1 \cdot (K_2 - K_1)}\right], \quad \lambda_2 = \frac{-k_B \cdot K_2 + k_B \cdot k_C}{K_2 \cdot (K_2 - K_1)} \tag{7}$$

$$\frac{M_\infty}{M_0} = \frac{k_B \cdot k_C}{K_1 \cdot K_2} \tag{8}$$

$$K_1 = k_B + k_{v1}, \quad K_2 = k_C + k_{v2} \tag{9}$$

M_0 is the initial sample mass on ash free basis; M_∞ is the final char yield [C] when time is sufficiently long. M/M_0 can be determined experimentally by:

$$\left(\frac{M}{M_0}\right)_{\text{exp}} = \frac{m_{\text{TGA}} - m_{\text{ash}}}{m_0 - m_{\text{ash}}} \tag{10}$$

where m_0 is the initial sample mass, m_{ash} is mass of ash in the sample and m_{TGA} is the mass measured by TGA as a function of time.

Di Blasi and Lanzetta [4] used graphical method to determine kinetic parameters by taking logarithm of Eq. (5).

$$\ln\left(1 - \frac{M_0 - M}{M_0 - M_{B^*}}\right) = -K_1 \cdot t \tag{11}$$

$$\ln\left(1 - \frac{M_{B^*} - M}{M_{B^*} - M_\infty}\right) = -K_2 \cdot (t - t^*) \tag{12}$$

where t^* is demarcation time, which separates the first and the second step. Consequently, M_{B^*} is the maximum value of the reaction intermediate mass, which occurs at time t^*. If the left side of Eqs. (11) and (12) is plotted against time for different temperatures, K_1 and K_2 can then be obtained from the slope of these sets of straight lines. Arrhenius plots are then used to get activation energies, Ea, and pre-exponential factors, A.

$$ln\, k = \ln(A) - \frac{\text{Ea}}{RT} \tag{13}$$

Prins et al. [12] mentioned that an exact demarcation time is difficult to establish for their results due to overlapping of the reaction steps. They used a numerical approach (MATLAB) to fit all kinetic parameters by minimizing the sum of squares function:

$$F = \sum_i \left[\left(\frac{M}{M_0}\right)_{\text{exp},i} - \left(\frac{M}{M_0}\right)_{\text{theor},i}\right]^2 \tag{14}$$

Different from Di Blasi and Lanzetta [4], bigger particle size (0.7–2.0 mm) and a much lower heating rate (10 °C min^{-1} to reach the isothermal part) was used in the experiments to obtain the kinetic parameters. However, the model fit the results obtained with the higher heating rate (100 °C min^{-1} at 260 °C) well in the first 14 min.

Repellin et al. [11] proposed that torrefaction is kinetically controlled and neglected heat transfer within wood chips in their study, because the time taken for the center of a wood chip to reach the temperature imposed at the surface of these chips is short compared to the heating rate and the residence time of torrefaction (e.g. at 200 °C, this characteristic time was 8 s for beech and 11 s for spruce). It was also concluded that for a residence time of more than 20 min, the anhydrous weight loss (AWL) depends almost entirely on the torrefaction temperature, because AWL is composed of two stages. The first stage is completed within 20 min with a rapid increase, the second one matches with a slow increase. They used activation energies found in the literature and adjusted kinetic constants for the three models to fit the calculated weight loss to the experimental data using a minimization of least squares method. The models used were a global one-step reaction model, a Di Blasi and Lanzetta model [4], and a Rousset model [14]. The Rousset model assumes that lignin and cellulose hardly react; hence the decomposition of hemicelluloses is the reason for the overall AWL of wood. However, Repellin et al. only compared the final AWL with experimental results; no comparison was conducted on the degradation of wood as a function of time.

Chen and Kuo [10] analyzed the thermal decompositions of the three constituents (hemicelluloses, cellulose and lignin) separately using TGA at 200–300 °C with 1 h residence time. Kinetic parameters (activation energy, pre-exponential factor and reaction order) were derived by applying a global one-step reaction model to the weight loss curve for these three constituents. With the assumption of no interaction among hemicelluloses, cellulose and lignin, the torrefaction of a mixture of these constituents can be described by the superimposed kinetics. The limitation of this model is that the heating period is not taken into account, and that the conversion of the components, especially hemicellulose and xylan, is already as high as 70% at the beginning of torrefaction at 300 °C. So the interpretation of the data lacks an important part of the whole process. And hence the use of this model will be limited if different heating rates are applied. Moreover, as the assumption of a constant ratio of char to volatile yields is made; one-step mechanisms cannot be applied to predict product distribution [4].

Therefore, the present study uses a two-step reaction in series model as shown in Eq. (1) and includes the non-isothermal part of torrefaction in the model. Wheat straw sample (<0.09 mm) was tested on TGA at heating rates of 10 and 50 °C min^{-1} to obtain intrinsic kinetic parameters. Afterwards this model and parameters were examined by comparing the residual mass predicted by the model and experimental data from a batch scale reactor. Secondly, devolatilization of wheat straw during torrefaction (at 250 and 300 °C) was studied by coupling a mass spectrometer with the TGA and detecting the gas products *in situ*. The relative quantity of each gas product from the two torrefaction temperatures was also compared. The objective of this study is to develop a kinetic expression that can predict the mass loss and gas evolution during torrefaction of wheat straw under real production conditions.

2. Experimental

2.1. Materials

The wheat straw used in this study is from winter wheat (*Triticum aestivum* L.), which was the most grown wheat species in Denmark in 2008. The straw was cut by hand in the field on the island of Funen, Denmark (55°21′N, 10°21′E) in August 2008, and stored indoors packed in paper bags. Prior to the TGA experiment, wheat straw were milled and particles smaller than 90 μm were collected. The cell wall composition and proximate analysis of the wheat straw raw material are listed in Table 1, and detailed descriptions of the analysis methods can be found in previous work [3,15].

2.2. Thermogravimetric analysis

Torrefaction of wheat straw (in the range of 250 and 300 °C) at heating rates of both 10 and 50 °C min^{-1} were carried out on a TGA (TG 209 F3, NETZSCH, Germany) with a nitrogen flow rate of 40 cm^3 min^{-1}. Sample weight varied from 3 to 5 mg, and ceramic crucible was used for the test. In each test, the sample was first heated up to 105 °C at 20 °C min^{-1} and held for 3 min for complete drying, then heated to the desired torrefaction temperature and held for 90 min. Afterwards, purge gas was switched from nitrogen to air and the sample was heated to 850 °C at 50 °C min^{-1}, and kept at this temperature for 5 min for complete combustion. The residual mass is the ash content, and data was obtained using Eq. (10). Two tests were conducted for each condition, and good reproducibility was achieved.

2.3. Thermogravimetric/mass spectrometric analysis

Torrefaction tests were also carried out using a thermal analyzer (STA 409, NETZSCH, Germany) in the TGA/DSC configuration mode. Prior to the experiment, wheat straw particles were dried in the oven at 100 °C overnight. Approximately 10 mg of the sample was placed on the microbalance and heated at 10 °C min^{-1} under 50 cm^3 min^{-1} argon, to a final temperature of 250 or 300 °C, and kept at this temperature for 1 h. Evolved gas was analyzed online by a quadrupole mass spectrometer (QMS 403 C, NETZSCH, Germany) coupled to the TGA. In order to prevent condensation of the evolved gas, the transfer line and inlet system of QMS was kept at ca. 300 °C. A small portion of the evolved gas together with the purge gas was led to the ion source of the mass spectrometer, since the pressure drops from atmospheric pressure in the TGA down to high vacuum in the QMS.

The analysis was focused on selected ions (m/z), in particular those which had been detected with high intensity. Since it is difficult to assign a given fragment to a single compound without confirmation by complimentary methods, the main detected m/z values were associated with the chemical species that are commonly present in gas products of wheat straw torrefaction or early stages of pyrolysis. A maximum number of 64 ions could be monitored as a function of time. The mass spectrometric intensities were normalized by the initial sample mass, and the background was subtracted. In order to compare the relative intensity of gas products at different temperatures, the signals were further normalized by the total intensity current (TIC) of the experiment [16]. However no specific response factors were applied. In order to reach the most reasonable association, the ion traces of both parent and fragment ions of most species have been considered. Furanes and phenols (tar), e.g. furfural and guaiacol, were not detected.

The quantification analysis of gaseous products released during torrefaction was only performed for H_2O in this study based on the methods used by Tihay and Gillard [17]. The concentration of H_2O was directly deduced from the ion intensities by:

$$[H_2O] = \frac{I_{18}}{F_A} \tag{15}$$

where I_{18} is the ion intensity for m/z 18 (H_2O), F_A is the calibration factor for H_2O. Correction due to $^{36}Ar^{2+}$ was not required.

2.4. Torrefaction in batch scale

In order to verify the model and kinetic parameters from the TGA test, torrefaction of wheat straw was conducted in a batch scale reactor as shown in Fig. 1. For each test, wheat straw (whole stalk, about 50 g) was first dried in the oven at 104 °C for 24 h prior to the torrefaction, and subsequently placed in an air tight metal reactor (15 cm × 31 cm × 10 cm) with nitrogen gas in and outlet, and a thermocouple centered in the reactor. The reactor was placed in an oven (type S 90, Lyngbyovnen, Denmark) with heating rate of 6 °C min^{-1}. Nitrogen flow was adjusted to 500 cm^3 min^{-1}, and a heater was used for gas outlet to avoid condensation. Torrefaction was carried out at temperatures spanning from 200 to 300 °C for about 2 h residence time (from the thermocouple inside the reactor reached the torrefaction temperature until the start of cooling down period). Ash content was determined by placing the samples in a muffle furnace at 550 °C for 3 h. Before the measurement, sample crucibles were ashed and dried. Two measurements were taken for each condition.

3. Results and discussion

3.1. Thermal decomposition characteristics

The differential thermogravimetric (DTG) curves at 250 °C and 300 °C are shown in Fig. 2, which allows observing the different torrefaction stages. The first peak between 50 °C and 150 °C is usually called drying stage, and corresponding to the vaporization of moisture, to the desorption of water and to the emission of volatile organic compounds [17]. The shoulder around 280 °C during torrefaction at 300 °C can be attributed to the hemicellulose degradation. The maximum peak, which occurs when temperature reaches 300 °C, corresponds to the main step of cellulose degradation (depolymerization). No shoulder is observed for torrefaction conducted at 250 °C, which means the reaction temperature of 250 °C is not high enough for the degradation of cellulose. This is in agreement with the conclusion drawn from our early work [3], where the degradation temperature of cellulose in wheat straw

Table 1
Chemical and proximate analysis (d.b.) of oven dried wheat straw.

	Cell wall composition			Proximate analysis			
	Lignin	Cellulose	Hemicellulose	Moisture	Volatiles	Fixed carbon	Ash
Wheat straw	20.3	34.0	26.5	1.35	74.78	19.23	4.6

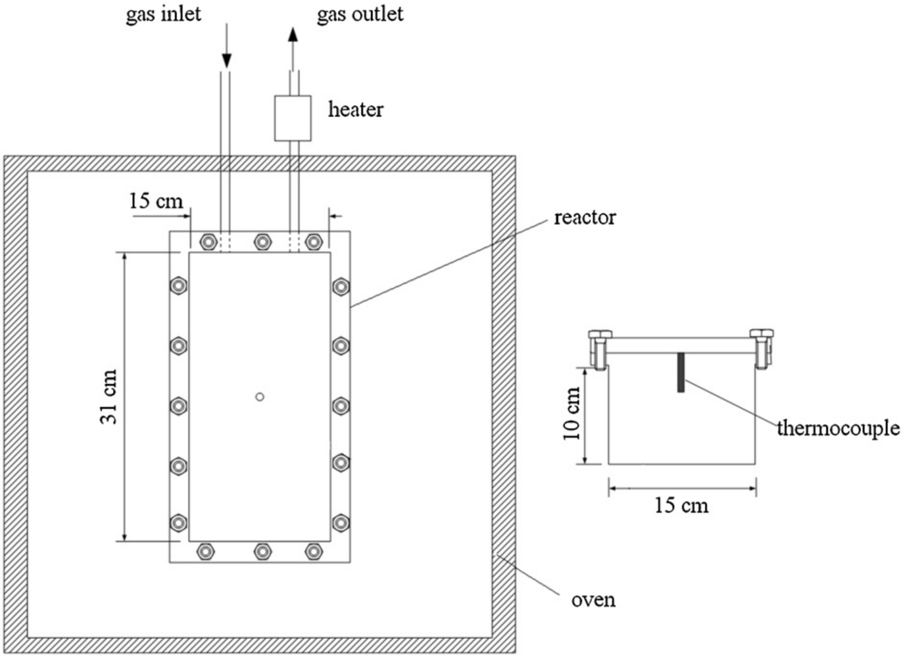

Fig. 1. Drawing of the torrefaction reactor.

was found to be between 270 and 300 °C. This also confirms the hypothesis of two-step reaction in serial models.

3.2. *Kinetic model for torrefaction*

The two-step reaction series model, as shown in scheme (1), was chosen for this study. In contrast to Di Blasi and Lanzetta [4], slow heating rate was used in this study to avoid intra-particle temperature gradients. Therefore, weight loss during heating stage needs to be taken into account when deriving the kinetic parameters from the isothermal stage:

$$\text{at } t = 0, \quad [A] = [A]_0, \quad [B] = [B]_0, \quad [C] = [C]_0$$

Integration of Eqs. (2)–(4) with the above mentioned initial conditions gives:

$$[A] = [A]_0 \exp(-K_1 t) \tag{16}$$

$$[B] = \frac{k_B[A]_0}{K_1 - K_2}\,[\exp(-K_2 t) - \exp(-K_1 t)] + [B]_0 \exp(-K_2 t) \tag{17}$$

$$[C] = [C]_0 + \frac{k_C\,(k_B[A]_0 + K_1[B]_0)}{K_1 K_2} + \frac{k_B k_C [A]_0 \exp(-K_1 t)}{K_1\,(K_1 - K_2)} - \frac{k_B k_C [A]_0 \exp(-K_2 t)}{K_2\,(K_1 - K_2)} - \frac{k_C [B]_0 \exp(-K_2 t)}{K_2} \tag{18}$$

$$\left(\frac{M}{M_0}\right)_{\text{theor}} = [A] + [B] + [C] \tag{19}$$

A schematic drawing of the algorithm taking into account the chemical composition change at the onset of the isothermal period is shown in Fig. 3. In the first iteration it was assumed that the entire solid is A, with no B and C. With this initial assumption and a starting guess of k_B, k_{V1}, k_C, k_{V2}, which were based on values found from [12], nonlinear optimization using the MATLAB (version R2008b) command ‘lsqcurvefit’ was made with the default tolerance settings. The ‘lsqcurvefit’ is based on the Niedler–Mead optimization algorithm and used to minimize the root mean square of the difference between the calculated and experimental data. Following this, at each temperature the four pre-exponential factors (A) and activation energies (Ea) were calculated by means of Arrhenius plot

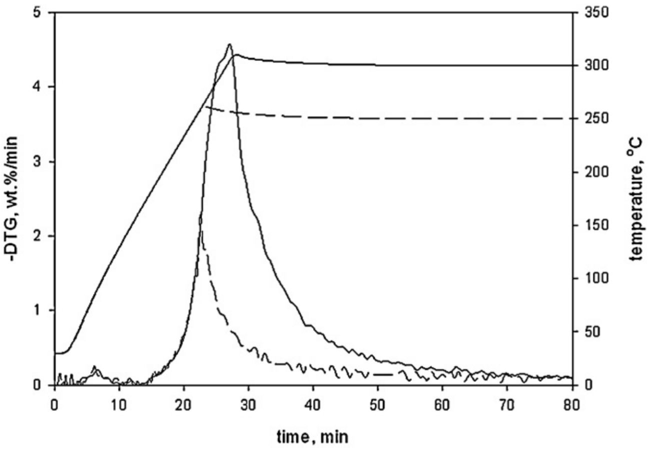

Fig. 2. Temperature and DTG profile of wheat straw torrefied at 250 °C (dash line) and 300 °C (solid line) at heating rate of 10 °C min^{-1}.

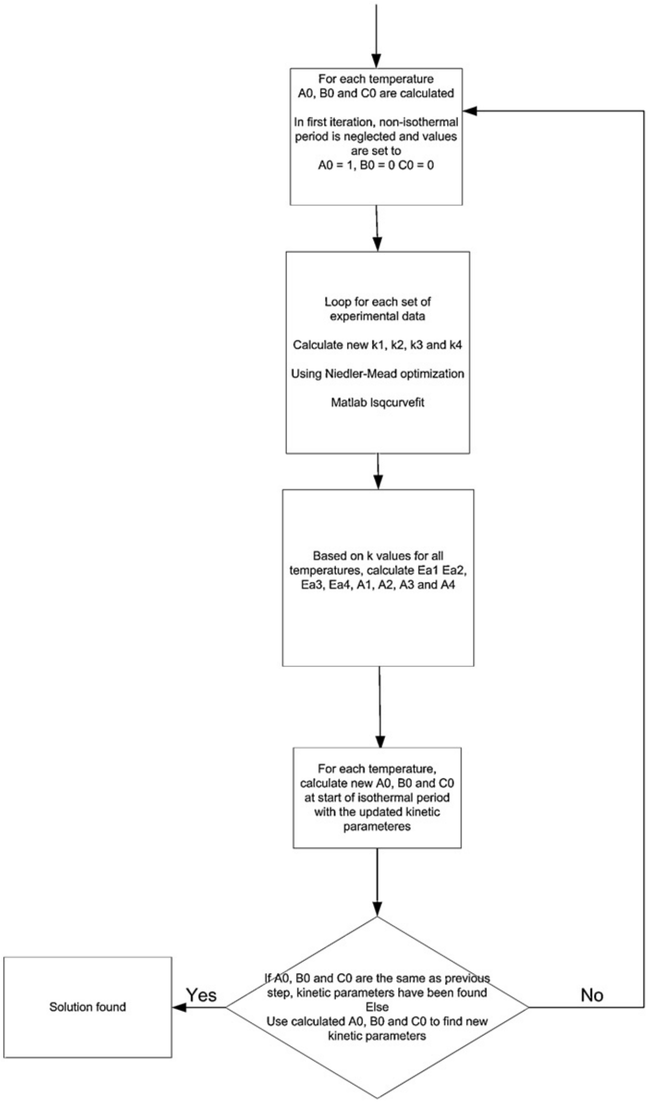
For each temperature
A0, B0 and C0 are calculated
In first iteration, non-isothermal period is neglected and values are set to
A0 = 1, B0 = 0 C0 = 0
Loop for each set of experimental data
Calculate new k1, k2, k3 and k4
Using Niedler-Mead optimization
Matlab lsqcurvefit
Based on k values for all temperatures, calculate Ea1 Ea2, Ea3, Ea4, A1, A2, A3 and A4
For each temperature, calculate new A0, B0 and C0 at start of isothermal period with the updated kinetic parameteres
If A0, B0 and C0 are the same as previous step, kinetic parameters have been found
Else
Use calculated A0, B0 and C0 to find new kinetic parameters
Yes
No
Solution found

Fig. 3. Diagram of algorithm used in MATLAB for calculating kinetic parameters of wheat straw torrefaction.

as shown in Eq. (13). With these calculated values the initial concentration of the isothermal period for *A*, *B*, and *C* can be obtained, and then used as input for the optimization. The calculations were done by numerical solution of the three coupled first order differential equations, as shown in Eqs. (2)–(4). To account for the heating rate, the chain rule was used to transform the equations into the temperature dependent form shown in Eqs. (20)–(22). From the second iteration and onwards the calculated *A* and Ea were used to provide the starting guess for the Niedler–Mead optimization. The procedure was repeated until stable values for the *A* and Ea were reached, as shown in Fig. 4.

$$\frac{d[A]}{dT} = \left(\frac{dt}{dT}\right) \cdot \left\{-(k_B + k_{v1})[A]\right\} = \frac{1}{\beta} \cdot \left\{-(k_B + k_{v1})[A]\right\} \tag{20}$$

$$\frac{d[B]}{dT} = \frac{1}{\beta} \cdot \left\{k_B[A] - (k_C + k_{v2})[B]\right\} \tag{21}$$

$$\frac{d[C]}{dT} = \frac{1}{\beta} \cdot \left\{k_C[B]\right\} \tag{22}$$

where β is the heating rate in °C s^{-1}.

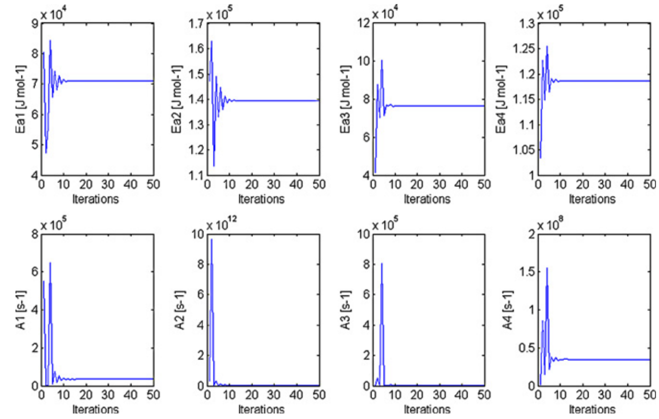

Fig. 4. Plot of activation energies (Ea) and pre-exponential factors (*A*) from each iteration when deriving kinetic parameters for k_B, k_{V1}, k_C, k_{V2} (from left to right).

3.3. Kinetic parameters and model verification

The kinetic parameters obtained by fitting the experimental data at 250, 260, 275 °C (at heating rate of 10 °C min^{-1}) and at 250, 260, 275, 280 (at heating rate of 50 °C min^{-1}) are as follows:

$$k_B = 3.48 \times 10^4 \exp\left(\frac{-70999}{RT}\right) \tag{23}$$

$$k_{v1} = 3.91 \times 10^{10} \exp\left(\frac{-139460}{RT}\right) \tag{24}$$

$$k_C = 4.34 \times 10^3 \exp\left(\frac{-76566}{RT}\right) \tag{25}$$

$$k_{v2} = 3.48 \times 10^7 \exp\left(\frac{-118620}{RT}\right) \tag{26}$$

where *k* is the reaction rate constant in unit of s^{-1}, *T* is the temperature in K, and *R* is the universal gas constant in J mol^{-1} K^{-1}. In agreement with literature, the first step is much faster than the second step. Solid yields for the two reaction steps decreased from 85% and 66% at 250 °C to 61% and 46% at 300 °C, respectively.

In order to verify the model, experimental data were compared with the model results for both the non-isothermal part (heating period from 200 °C to final torrefaction at both heating rates) and isothermal part. Due to the similarity, only results from 10 °C min^{-1} are shown in Fig. 5 part (a). Instead, a multiple-step torrefaction was run from 200 °C to 270 °C at different heating rates and held at 270 °C for 1 h. The model and experimental results are shown in Fig. 5(b). It can be seen the model described the reaction accurately.

The model was also tested on torrefaction of wheat straw conducted in a batch reactor, as shown in Fig. 1. The temperature recorded in the center of the reactor was used as the input for the model to calculate the residual mass, assuming heat transfer from the wheat straw surface to the center is much faster than the heating rate of the oven. Model and experimental results are shown in Fig. 6. There is a good correlation between model results and experimental data.

3.4. Gas evolution with MS analysis

Gas products detected during torrefaction of wheat straw based on selected ions were water (18), carbon monoxide (28), formic acid (46, 45), formaldehyde (30, 29), methanol (31, 32), acetic acid (43, 45, 60), carbon dioxide (44), methyl chloride (50, 52). Traces of hydrogen sulfide (34) and carbonyl sulfide (60, 48) were also found. In addition, relatively large quantities of simple aliphatic hydrocarbons were apparently present, C_xH_y and C_xH_{2x} (15, 27, 39, 41).

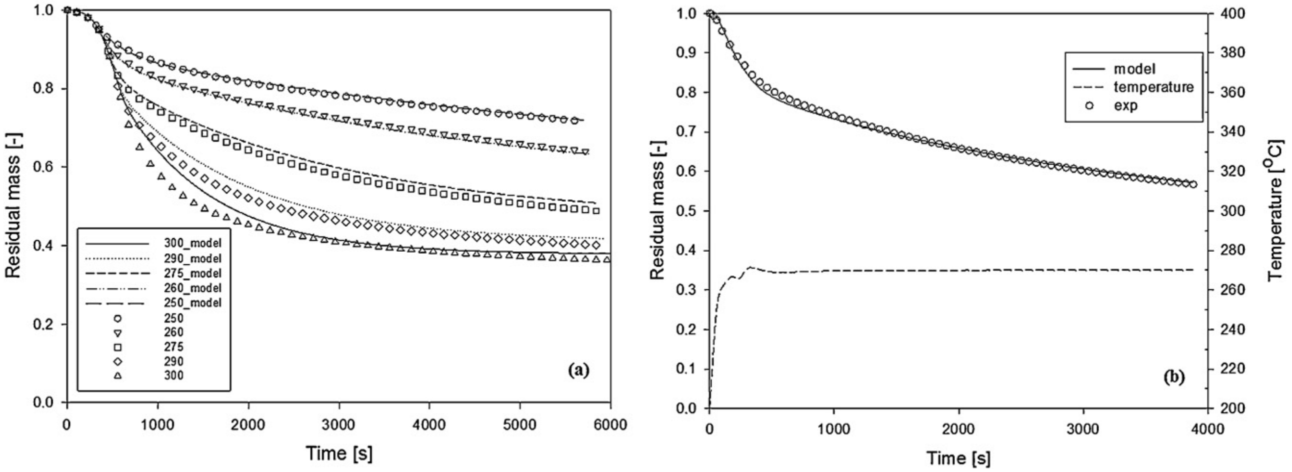

Fig. 5. Experimental and modeled relative weight (on ash free basis) of wheat straw vs. time for (a) at heating rate of 10 K min^{-1}. (b) Multiple-step heating at various rates. Starting weight is defined at 200 °C; heating period from 200 °C to desired torrefaction temperature is included in the plot.

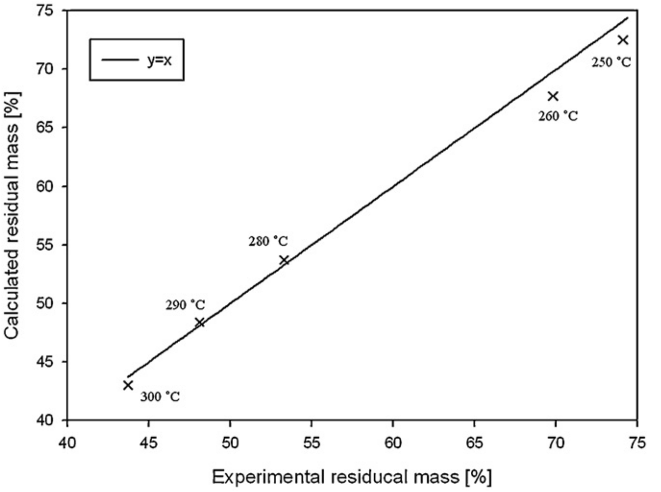

Fig. 6. Correlation between experimental residual mass obtained from torrefaction of wheat straw in a batch reactor and calculated results from the model. Both results are on dry and ash free basis.

Table 2
Fraction of wheat straw overall mass loss at two stages, and calculated mass fraction of water evolved during torrefaction after the drying stage.

%	300 °C	250 °C
Mass loss at 10 min	0.66	0.67
Mass loss at 81.5 min	57.95	21.59
H_2O released from 10 to 81.5 min	26.00	7.94

Since no signals other than water was observed during the early stage (<150 °C), the total weight loss in this period can be attributed to the release of water (the first peak of $m/z = 18$ in Fig. 7). Based on Eq. (15), the cumulative water evolution during torrefaction after drying stage (the second peak of $m/z = 18$), $m_{H_2O,2nd}$, can be calculated by Eq. (27) and results are shown in Table 2. It can be seen that at 300 °C, evolution of water (26.66%) accounts for almost half of the overall mass loss (57.95%). Similar results were reported by Prins et al. [18] that a mass fraction of 5.5% released from straw when torrefied at 250 °C for 30 min was water and water released from willow when torrefied at 300 °C and 250 °C was 13% and 7%, respectively.

$$m_{H_2O,2nd} = m_{H_2O,1st} \times \frac{\int_{10\,\mathrm{min}}^{81.5\,\mathrm{min}} I_{18}}{\int_{0\,\mathrm{min}}^{10\,\mathrm{min}} I_{18}} \qquad (27)$$

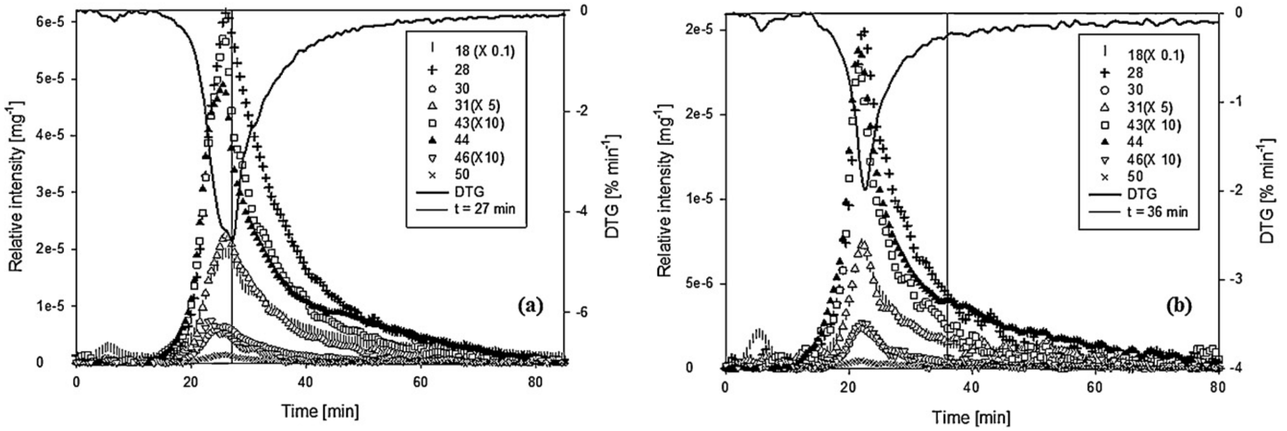

Fig. 7. DTG and MS curves of wheat straw torrefied at 300 °C (a) and 250 °C (b). The straight line refers to the time when yield of the intermediate solid product '*B*' reaches the maximum.

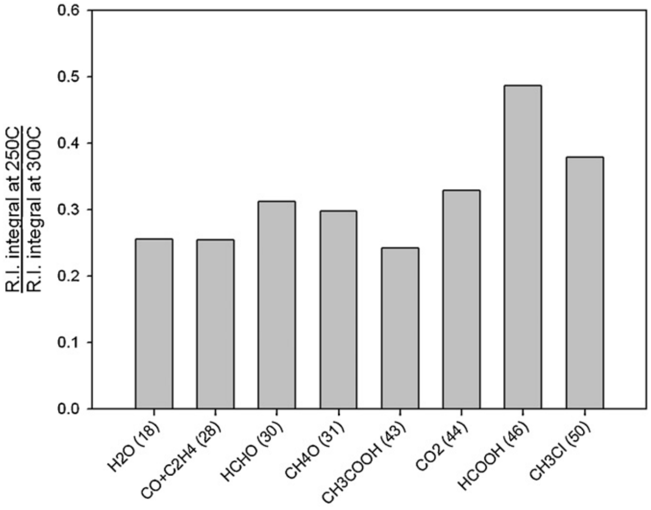

Fig. 8. Ratio of each gas product released from wheat straw at 250 and 300 °C by calculating the relative intensity (RI) integral over the period from 200 °C until the end of torrefaction.

Fig. 8 indicates the relative quantities of each gas released from torrefaction at temperatures of 250 and 300 °C for a residence time of 1 h. It can be seen that the quantities of most of the gas products released at 250 °C was about 30% of the gasses released at 300 °C, except for formic acid (46). It means that formic acid is preferentially released at lower temperatures compared to the other gases. This phenomenon can also be observed from the 300 °C data in Fig. 7, where the peak of this compound appeared before the other products.

4. Discussion

Fig. 9 shows the change of A, B, and C at torrefaction temperatures of 250 and 300 °C with a heating rate of 10 °C min^{-1} from 200 °C. At a torrefaction temperature of 300 °C, the isothermal part of torrefaction starts at 600 s, where $[A]_0$ is as low as 4%. So it is not reasonable to assume that only A is present at the beginning of the reaction with a low heating rate such as 10 °C min^{-1} as in [12]. In order to simulate the model with such assumption, 1 iteration instead of 50 was run to derive the kinetic parameters. A comparison of model results and experimental data are shown in Fig. 10.

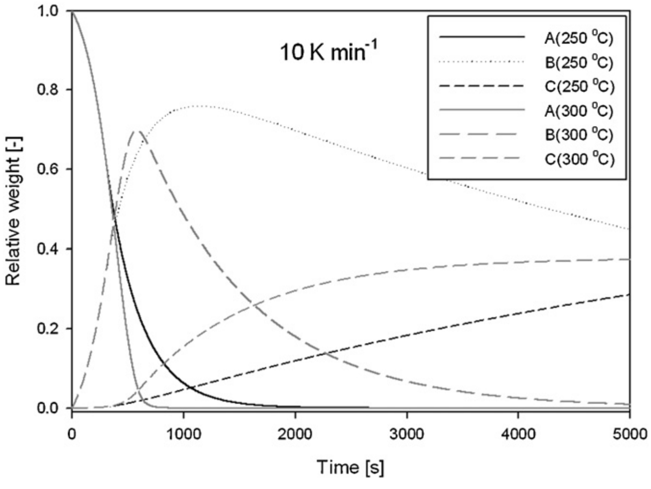

Fig. 9. Yields of A, B, and C at torrefaction temperature of 250 and 300 °C and heating rate of 10 °C min^{-1}. Starting weight defined at 200 °C, heating period from 200 °C is included in the plot.

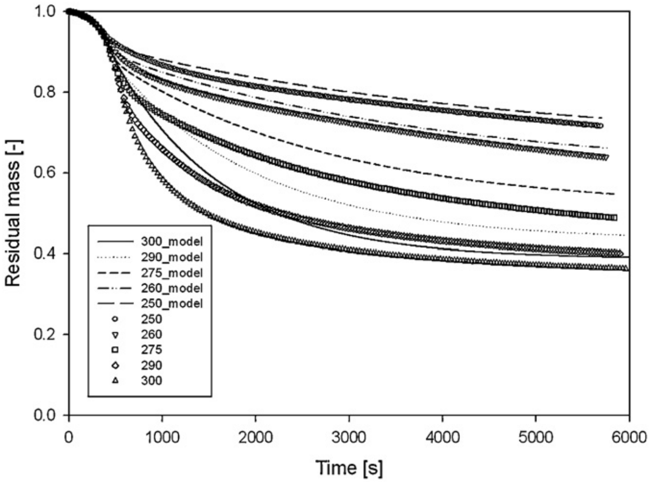

Fig. 10. Same experimental results as in Fig. 5 part (a), but with modeled relative weight using kinetic parameters from only one iteration.

In comparison with Fig. 5, which shows the model results using parameters from 50 iterations, it can be seen that the parameters from 50 iterations gives a better fit to the experimental data.

In this study, experimental data at both heating rates (10 and 50 °C min^{-1}) were used to derive the activation energies (Ea) and pre-exponential factors (A), because model with these parameters gives best fit to most experimental results. It can be seen in Fig. 5 that at higher temperature the agreement between model and experimental data is not as good as at lower temperature. This is because the experimental data used to derive the kinetic parameters is only up to 275 °C for 10 °C min^{-1}, and 280 °C for 50 °C min^{-1}. The reason of not including experimental data above 280 °C is due to that the heating rate of the TGA is limited to 80 °C min^{-1}, and thus while being heated to high temperature (e.g. 300 °C) major fraction of A will already be transformed to B in initial non-isothermal phase of experiments. Another potential problem is the temperature overshooting when reaching the desired temperature in TGA, and the higher the set temperature (and/or the higher the heating rate) the larger the overshoot occurs. For example, the overshoot can be 10 °C for 290 °C with 50 °C min^{-1}. It was also found kinetic parameters obtained by including these experimental data do not fit well with 10 °C min^{-1} experimental data when applied to the model.

According to Fig. 9, the maximum yield of B ($[B]_{\max}$) is found at 580 and 1140 s for torrefaction temperatures of 300 and 250 °C, respectively. At 300 °C, $[B]_{\max}$ locates close to the end of first step reaction and the early stage of the second step reaction, since the yield of A decreases to almost zero and the yield of C just starts to increase from 0. While for 250 °C $[B]_{\max}$ is reached during the second step. The vertical straight lines in Fig. 7 correspond to 580 and 1140 s after reaching 200 °C. Correspondingly, most gases were released before reaching the $[B]_{\max}$ for 250 °C, while for 300 °C more than half of the gas products were released after reaching the $[B]_{\max}$.

However, when applying the model to a real torrefaction facility, there could be limitations from heat transfer when biomass in other forms (e.g. logs, chips, etc.) or other kinds (e.g. biomass with different compositions that may generate heat during torrefaction) are used as feedstock. In this case, a heat transfer model will need to be coupled to the existing kinetic model for the mass loss calculations.

5. Conclusion

A two-step first order reaction in series model was used to study the kinetics of wheat straw torrefaction in a TGA setup. In contrast to other studies, which obtained the kinetic parameters from the isothermal part of torrefaction by neglecting the degradation of sample during the heating period, this paper took the mass loss during the heating period into account when deriving the parameters. The results show that parameters obtained in this way are in better accordance with the experimental results. Torrefaction of wheat straw was also conducted in a batch scale reactor at a much lower heating rate; a model with kinetic parameters obtained from TGA gave good prediction of residual mass at the end of the reaction. It means the mass yield and gross chemical state of solids in the real torrefaction facility can be predicted by simply knowing the temperature history of the sample. By analyzing the gas evolution *in situ*, water, carbon monoxide, formic acid, formaldehyde, methanol, acetic acid, carbon dioxide, methyl chloride, and traces of hydrogen sulfide, carbonyl sulfide were found at both 250 and 300 °C. At 300 °C, evolution of water accounts for almost half of the overall mass loss.

Acknowledgements

This work was financially supported by ENERGINET.DK and the ForskEL program (Project 2009-1-10202, Torrefaction of Biomass). The authors express their appreciation to Freddy Christensen, Kristian Estrup, Erik Hansen for the assistance of building the torrefaction reactor and to Tobias Thomsen for performing the torrefaction. Thanks are also due to Tomas Fernqvist for conducting the cell wall composition analysis.

References

[1] M.J.C. van der Stelt, H. Gerhauser, J.H.A. Kiel, K.J. Ptasinski, Biomass upgrading by torrefaction for the production of biofuels: a review, Biomass Bioenergy 35 (9) (2011) 3748–3762.

[2] L. Shang, N.P.K. Nielsen, J. Dahl, W. Stelte, J. Ahrenfeldt, J.K. Holm, et al., Quality effects caused by torrefaction of pellets made from Scots pine, Fuel Processing Technology 101 (2012) 23–28.

[3] L. Shang, J. Ahrenfeldt, J.K. Holm, A.R. Sanadi, S. Barsberg, T. Thomsen, et al., Changes of chemical and mechanical behavior of torrefied wheat straw, Biomass Bioenergy 40 (2012) 63–70.

[4] C. Di Blasi, M. Lanzetta, Intrinsic kinetics of isothermal xylan degradation in inert atmosphere, Journal of Analytical and Applied Pyrolysis 40 (1997) 287–303.

[5] M. Stenseng, A. Jensen, K. Dam-Johansen, Investigation of biomass pyrolysis by thermogravimetric analysis and differential scanning calorimetry, Journal of Analytical and Applied Pyrolysis 5 (2001) 8–59, 765-780.

[6] D.K. Shen, S. Gu, K.H. Luo, A.V. Bridgwater, M.X. Fang, Kinetic study on thermal decomposition of woods in oxidative environment, Fuel 88 (6) (2009) 1024–1030.

[7] K. Ninan, Kinetics of solid state thermal decomposition reactions, Journal of Thermal Analysis and Calorimetry 35 (4) (1989) 1267–1278.

[8] L. Helsen, E. Van den Bulck, Kinetics of the low-temperature pyrolysis of chromated copper arsenate-treated wood, Journal of Analytical and Applied Pyrolysis 53 (1) (2000) 51–79.

[9] J.E. White, W.J. Catallo, Biomass pyrolysis kinetics: a comparative critical review with relevant agricultural residue case studies, Journal of Analytical and Applied Pyrolysis 91 (1) (2011) 1–33.

[10] W.H. Chen, P.C. Kuo, Isothermal torrefaction kinetics of hemicellulose, cellulose, lignin and xylan using thermogravimetric analysis, Energy 36 (11) (2011) 6451–6460.

[11] V. Repellin, A. Govin, M. Rolland, R. Guyonnet, Modelling anhydrous weight loss of wood chips during torrefaction in a pilot kiln, Biomass Bioenergy 34 (5) (2010) 602–609.

[12] M.J. Prins, K.J. Ptasinski, F.J.J.G. Janssen, Torrefaction of wood Part 1: weight loss kinetics, Journal of Analytical and Applied Pyrolysis 77 (1) (2006) 28–34.

[13] C. Branca, C. Di Blasi, Kinetics of the isothermal degradation of wood in the temperature range 528–708 K, Journal of Analytical and Applied Pyrolysis 67 (2) (2003) 207–219.

[14] P. Rousset, I. Turner, A. Donnot, P. Perré, The choice of a low-temperature pyrolysis model at the microscopic level for use in a macroscopic formulation, Annals for Forest Science 63 (2) (2006) 1–17.

[15] L. Shang, W. Stelte, J. Ahrenfeldt, J.K. Holm, R. Zhang, Y. Luo, et al., Physical and chemical property changes of 3 biomass fuels caused by torrefaction. Biomass Bioenergy (under review).

[16] A. Arenillas, F. Rubiera, J. Pis, Simultaneous thermogravimetric-mass spectrometric study on the pyrolysis behaviour of different rank coals, Journal of Analytical and Applied Pyrolysis 50 (1) (1999) 31–46.

[17] V. Tihay, P. Gillard, Pyrolysis gases released during the thermal decomposition of three Mediterranean species, Journal of Analytical and Applied Pyrolysis 88 (2) (2010) 168–174.

[18] M.J. Prins, K.J. Ptasinski, F.J.J.G. Janssen, Torrefaction of wood: Part 2: analysis of products, Journal of Analytical and Applied Pyrolysis 77 (1) (2006) 35–40.